

MULTIBODY FEM AND EXPERIMENTAL ANALYSIS OF THE TIMING SYSTEM OF I.C EIGHT-CYLINDER ENGINE

B.Umamaheswara Gowd¹

¹Professor

Department of Mechanical Engineering, JNTU College of Engineering (Autonomous), Anantapur,
dr_acreddy@yahoo.com

A. Chennakesava Reddy²

²Associate Professor

Abstract The dynamic behavior and the related stresses of the timing system of a eight cylinder engine has been investigated in this paper. The study has the goal to analyze and improve the performance of the entire system by means of parametric numerical models. With more details, an integrated FEM multibody analysis has been employed, which has taken into account both flexible and lumped parameters bodies. The numerical models have been validated by experimental testes regarding both static characterizations and modal analyses. As a results of numerical simulations the complete response of the system has been obtained at constant angular velocity and during transient phase from idle to maximum rpm of the engine.

1. INTRODUCTION

The timing system and its single units are often designed considering only fluid dynamic performance and are frequently based on existing architectures. The analytical instruments used are somewhat simplified, the system is seen as infinitely rigid and the preset laws of camshaft acceleration are not subsequently verified at the various operating engine speeds. The more elevated the specific power and revolution speeds of an engine, the more important it is that a complete dynamic analysis is carried out on the system, allowing the identification of any critical points and the analysis of possible modifications. Such critical areas can concern both the functionality of the system and the duration of components such as, for example, that of the timing belt or cam profiles. The analyses of such a complex system cannot, however, be made with classic techniques so that the use of numerical simulation programmes is indispensable [1–4].

The principle objective of the study is to analyze the feasibility of a parametric numerical model which, using integrated multibody finite element modeling (FEM), makes it possible to study the dynamic behavior of the timing system, considering the elasticity of the bodies and evaluating the stress, strain and vibrational states of the components under different operating conditions [5,6]. The need to determine with precision some of the more significant magnitudes for the dynamic simulation of the system, such as the deformability of the supports and the torsional and bending stiffnesses of the shafts, required a series of experimental trials. In particular, almost static strain gauge measurements, and bending and torsional strain measurements were made on the shafts. The system studied is that of a V8 engine.

2. CALCULATION MODELS

The numerical models were constructed using the ADAMS ENGINE calculation programme, which allowed the construction of complete models of the timing system (camshafts, valve trains, belts), and the NASTRAN calculation programme of MSC, by which it was possible to validate the models on the basis of experimental trials and also to analyze the stress and strain states of the various components. The different numerical models constructed were:

- a multibody model for the study of the single valve trains (Figure 1);
- a multibody model of the entire system relative to a camshaft main bearing;
- a complete multibody model of the entire timing system, consisting of four shafts, 40 valves and two toothed belts (Figure 2); and
- FEM models of the various components, with particular reference to the intake and exhaust shafts.

The modal approach was taken in considering the flexible bodies. The method used for modal synthesis is that implemented in ADAMS, developed by Craig and Bampton [7], which allows the number of generalized coordinates to be reduced to a minimum and provides greater freedom in the definition of the constraint conditions on the boundary points. Numerical-experimental modal analysis of the components allowed the generation of transfer files (.mnf) [8,9] for each body, modeling their flexible behavior. With the aim of lessening the degrees of freedom, a simplification was adopted where the shafts were reduced to equivalent concentrated parameter systems, taking into account only torsional behavior. The stiffnesses were measured experimentally, while damping was calculated for each individual spring as a fraction of the stiffness. Using an iterative procedure, these values were then corrected until a value was obtained for the damping of the entire shaft which was equal to that determined by free-body modal analysis (Figure 3, Table-1 and 2).

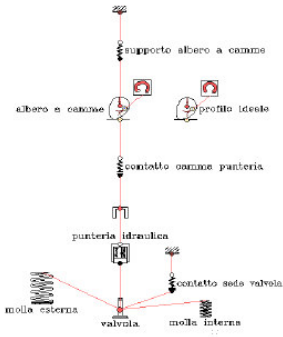


Figure 1. Single valve train model

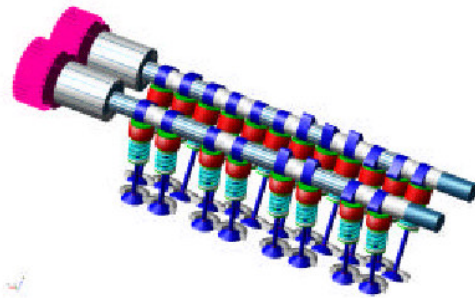
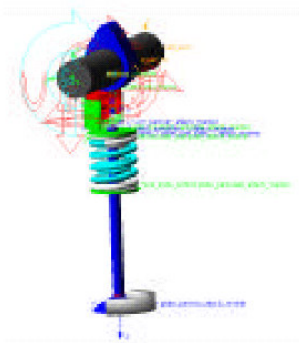


Figure 2. Complete valve train model

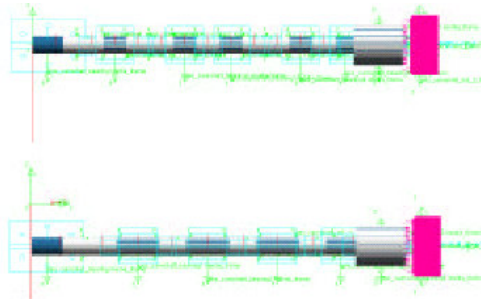


Figure 3. Concentrated parameter models of the intake and exhaust shafts

The numerical models of the camshafts, complete with pulleys and phase variator, caps and all the components of the single valve trains, were created by the discretisation of solid CAD 3D models (Figure 4). A modular construction technique was followed, constructing one component at a time and then assembling them all in a single file. As an example, the rendered representation of the intake camshaft, complete with pulley and dummy phase variator is shown. This is composed of 255630 solid tetrahedral elements with 4 nodes, and has a total of 59232 nodes (Figure 5).

Table –1: Bending trial on the shafts

SECTION OF SHAFT	FORCE [N]	DISPLACEMENT [µm]	STIFFNESS [N/mm]
INTAKE SPAN 63.1 mm	12000	83	144500
INTAKE SPAN 94.662 mm	12000	112	107100
EXHAUST SPAN 94 mm	12000	97	123700
LONG INTAKE SPAN (1 ^a vertical cam)	2000	1010	1830
LONG INTAKE SPAN (1 ^a cam at 90°)	2000	920	2073
LONG EXHAUST SPAN (1 ^a vertical cam)	2000	870	2298
LONG EXHAUST SPAN (1 ^a cam at 90°)	2000	893	2240

Table-2: Torsion trial

SECTION OF SHAFT	TORQUE [Nmm]	ROTATION [degrees]	STIFFNESS [Nmm/degree]	DISPLACEMENT [N s mm/degree]
BETWEEN INTAKE CAMS	432,000	0.330	1,307,309	1.31
BETWEEN EXHAUST CAMS	467,000	0.715	653,290	n. d.
BETWEEN INTAKE SUPPORTS	432,000	0.96	450,000	n. d.
BETWEEN EXHAUST SUPPORTS	467,000	0.537	870,000	n. d.
INTAKE CONVERTER-PULLEY	315,000	0.0365	8,655,422	8.66
EXHAUST CONVERTER-PULLEY	356,000	0.0412	8,655,422	n. d.



Figure 4. Solid parametric models of some system components

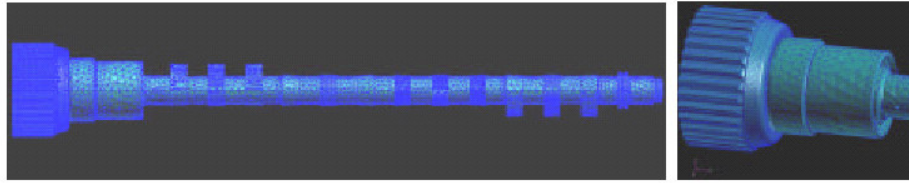


Figure 5. Intake shaft and detail of pulley and phase variator

The numerical modal analysis was performed using the Lanczos method [10] of the MSC-NASTRAN finite element programme. The file with the results processed using FEMAP gave the natural vibration modes and corresponding modal forms. Both FEM and multibody models were validated by varying the stiffness characteristics in such a way that an excellent agreement was obtained with the results of the experimental trials. With regard to the dynamic behavior, appropriate adjustments were made so that the non-damped modal forms were coincident with those determined experimentally.

3. EXPERIMENTAL TRIALS

Static and dynamic experimental trials were carried out. With static trials, using mechanical comparators and electrical resistance strain gauges, it was possible to determine the stiffnesses, and bending and torsional strains of the single segments making up the shafts. Measurement of the stress and strain states performed using strain gauges and comparators, had the aim of providing comparison values for the FEM model. A universal test machine equipped with appropriate clamps was used to apply external loads to the shafts.

Figures 6 and 7 show the loading, constraint and measurement schemes followed in the torsion and bending tests on the shafts. A summary of the trial results are reported in tables 1 and 2. The experimental modal analysis was performed suspending the shafts elastically, exciting them using an instrumented hammer (Brüel & Kjær) and measuring the response with a piezoelectric accelerometer (Brüel & Kjær). The signals were acquired and elaborated using a Data Physics DP420 spectrum analyser and STAR System software (GenRad/SMS Inc). For each of the two shafts, the analyses were repeated in two orthogonal planes to obtain the bending modal forms, placing the accelerometer at the extremity of the shaft. Specific trials were also performed to determine the torsional natural frequencies, placing the accelerometer circumferentially at the first cam.

Tables 3–5 show the values of the first six natural frequencies and the corresponding natural vibration modes of the intake shaft, with and without pulleys, and of the exhaust shaft. From the analysis of the results, it was possible to evaluate the influence the pulleys and phase converters have on the natural frequencies. A notable damping effect caused by the exhaust shaft phase converter can be seen, in particular on the first torsional natural frequency.

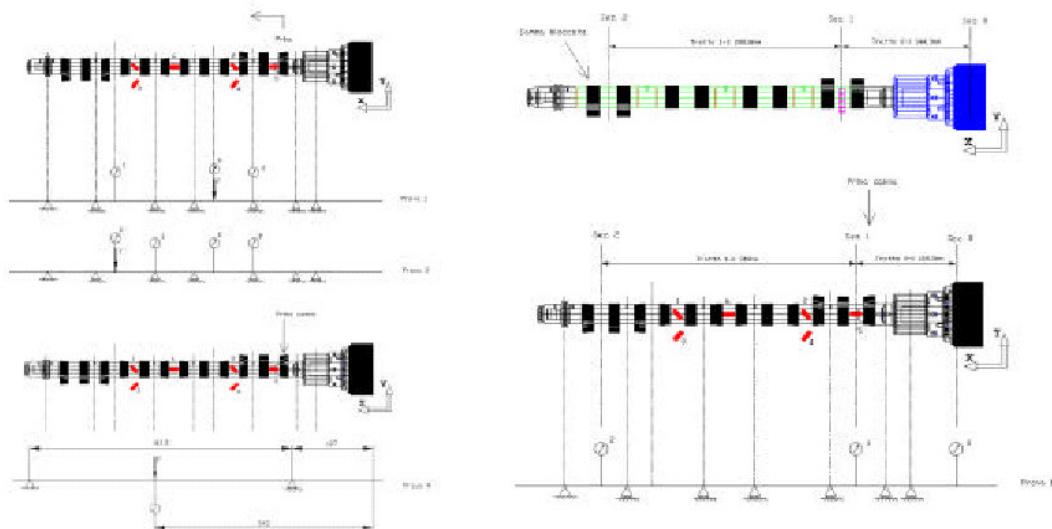


Figure 6. Load, constraint and measurement schemes in bending Figure 7. Load, constraint and measurement schemes in torsion

Table-3: Natural frequencies of the intake shaft with pulleys

Mode	Freq.[Hz]	Damp.[Hz]	Damp.[%]	Mag.	Phase
1	336.84	2.14	0.634	5720	170.7
2	949.55	3.02	0.318	5920	182.2
3	1620	9.46	0.583	28930	352.9
4	1890	3.04	0.161	10660	185.3
5	3030	4.57	0.151	274660	130.4
6	3770	6.47	0.172	357380	121.1

Table-5: Natural frequencies of the exhaust shaft with pulleys

Mode	Freq.[Hz]	Damp.[Hz]	Damp.[%]	Mag.	Phase
1	336.3	2.78	0.827	4830	357.7
2	897.3	17.31	1.93	438.84	303.6
3	1460	101.45	6.92	23330	173.7
4	1770	48.74	2.75	4320	307.9
5	2740	123.61	4.51	75780	208
6	3270	167.33	5.12	43320	44.7

Table-4: Natural frequencies of the intake shaft without pulleys

Mode	Freq.[Hz]	Damp.[Hz]	Damp.[%]	Mag.	Phase
1	390.52	2.72	0.696	7320	180.3
2	1100	3.12	0.284	5580	178.1
3	1840	9.88	0.536	34450	356.1
4	2140	2.77	0.129	6400	204.2
5	3460	11.64	0.337	88570	324.9
6	4770	34.96	0.732	13710	173.3

Table-6: Harmonics in resonance

ORDER	AMPLITUDE [Nm]	ENGINE SPEED [rpm]
20	0.3	4506
24	0.11	3755
28	0.13	3219
32	0.09	2816

4. ANALYSIS OF RESULTS

Of the large quantity of data which could be considered, relating to different models of increasing complexity, for brevity, it was decided to highlight the dynamic behaviour of the camshafts, with particular reference to the intake shaft, decidedly less damped than the exhaust shaft. Figure 8 shows the trends of the turning moment below the first cam as a function of the angular position of the shaft, obtained at 500 rpm, 3755 rpm and 4200 rpm (maximum shaft rotation speed). The values obtained at 500 rpm correspond to those of an infinitely rigid shaft. Figure 10 shows the trends of the torque on varying the damping of the shaft, obtained, instead, at the point of greatest stress immediately before the pulley (where the modulus of resistance to torsion has the minimum value $Wt=2844 \text{ mm}^3$). It can be seen that while the first torsional frequency of the shaft is not excited at low speed, higher speeds provoke considerable vibration associated with this modal form.

Fourier analysis of the excitation couple and of the response, reported in Table-6 and Figure 11, show the phenomenon clearly. In the operating range, the first harmonic of the applied force to excite the torsional natural mode is the 24th. This is exactly in resonance with the speed of 3755 revolutions per minute; however the vibrations at maximum speed are slightly higher than these (Figure 9) because the applied force torque increases with the speed, in association with the increase in the force of inertia on the valve. Further, it can be seen that the torsional vibrations of the shaft do not induce substantially greater maximum torque values compared to the case of the rigid shaft. Nevertheless, they imply a number of cycles to fatigue which is almost an order of magnitude greater (Figures 9 and 10). The shear stress value corresponding to the moment reported in Figure 10 is 65 MPa, i.e. below the fatigue limit of the steel (40NiCrMo4 $\sigma_{sn}=482$, $\sigma_0=161$, $\sigma'_0=322$). From the functional point of view, angular vibrations occur with a maximum value of $15'$ producing errors of phasing which are altogether negligible (figure13). The results reported in Figures 9–13 were obtained using a model in which the shaft was schematised by only the masses and torsional springs. It was however preventatively verified that the first bending modal form of the shaft can be ignored: even schematising all the supports, such as carriages, which block the two transversal movements of the shaft, the natural frequency is around 9200 Hz, with the applied force producing practically no excitation (see Figure 12).

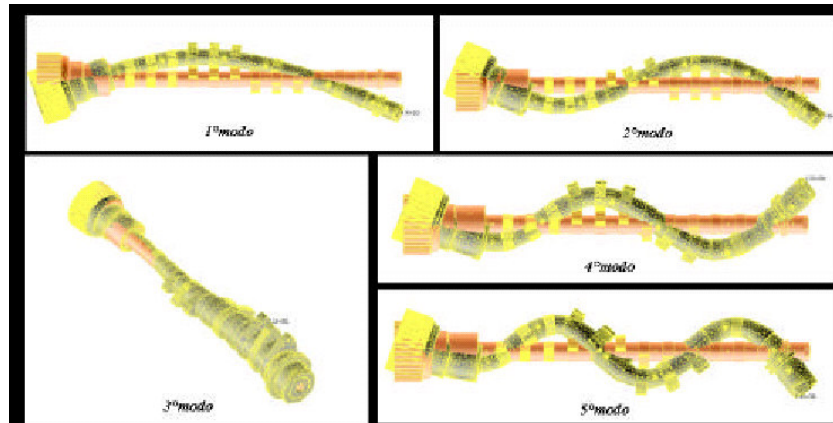


Figure 8 – 1st, 2nd, 3rd, 4th and 5th natural modes of the free structure (339.03 Hz; 977.75 Hz; 1682.4 Hz; 1938 Hz; 3314.9 Hz)

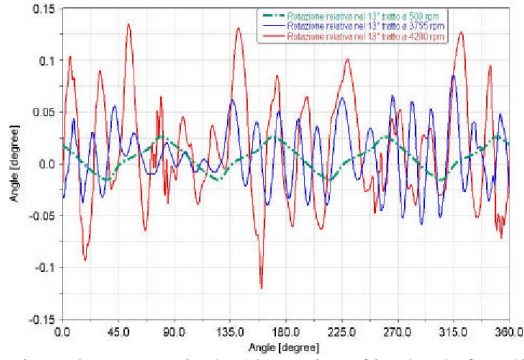


Figure 9. Moment in the 13th section of intake shaft at 500 rpm, 3755 rpm and 4200 rpm

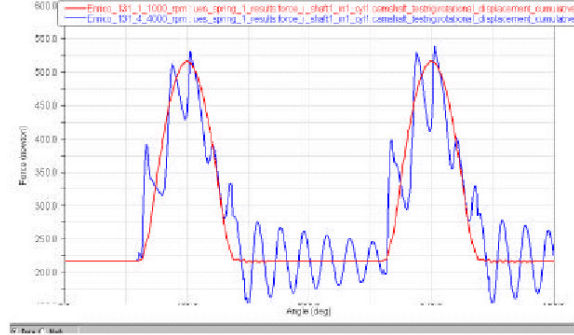


Figure 10. Moment in the 14th section of intake shaft at 3755 rpm

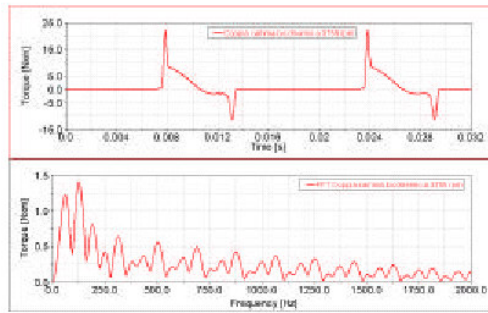


Figure 11. Torque of valve trains on the shaft at 3755 rpm

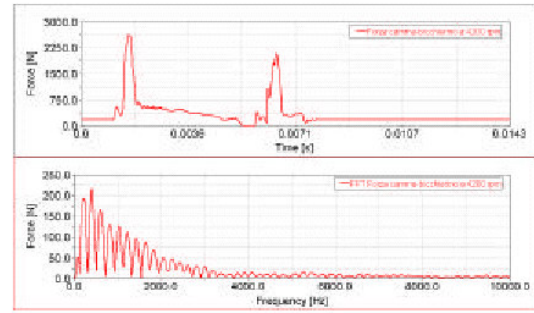


Figure 12. Force of valve trains on the shaft at 4000 rpm

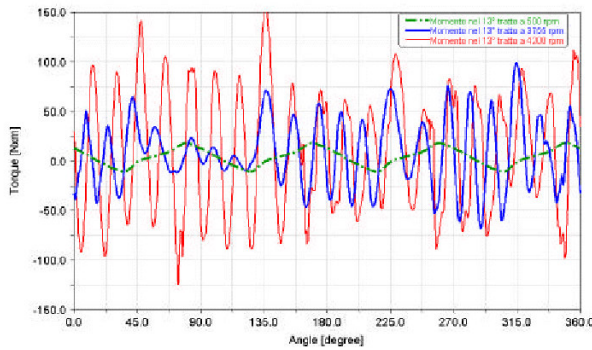


Figure 13. Relative rotation between the intake shaft extremities at 500 rpm, 3755 rpm and 4000 rpm

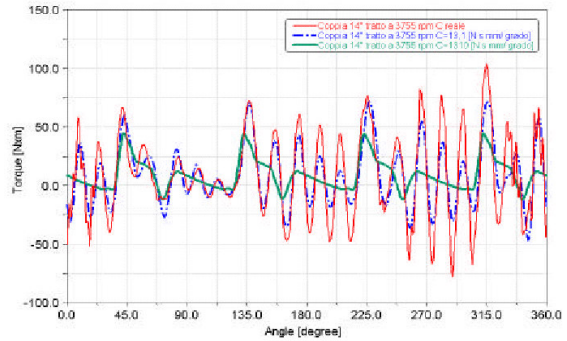


Figure 14. Internal spring load at minimum and maximum velocities

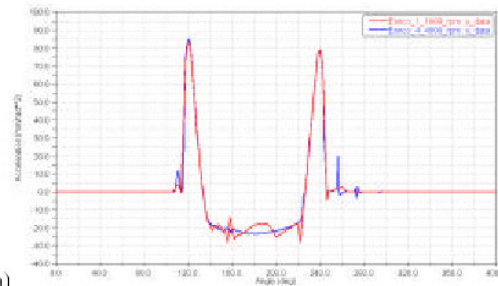
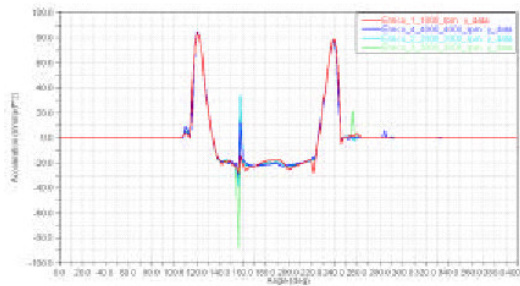


Figure 15. Acceleration along the axis of the valve of the plate top: (a) original spring; (b) variable pitch spring

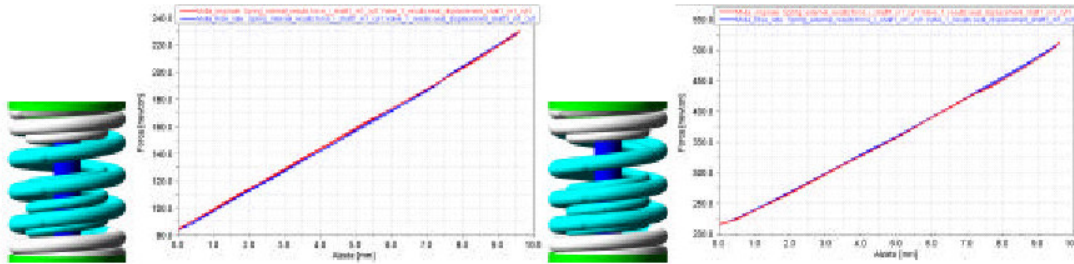


Figure 16. Stiffness of the original spring and the variable pitch spring

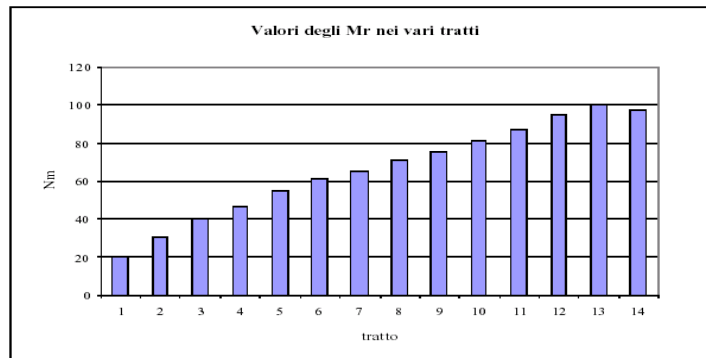


Figure 17 – Maximum moment in various sections

4.2 Phenomena of spring resonance

Another phenomenon to which attention should be drawn is that of the resonance of the internal valve spring (Figure 14). When the operating speeds of the engine shaft increase above 8000 rpm, the springs present evident limits from the dynamic viewpoint: their low internal damping values in fact result in brusque and unacceptable discontinuities in loading which, apart from making one turn of the spring impact with another (Figure 15), also have repercussions on the moving elements, provoking vibration of the entire valve train. Using a variable pitch spring (Figure 16), which maintains the same stiffness, it was shown that this phenomenon could be completely eliminated without altering the functionality of the system.

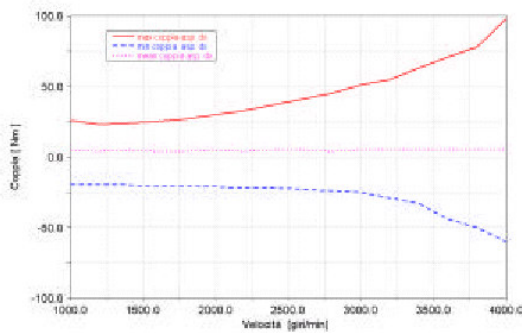


Figure 18– Moment in the 13th section during transient

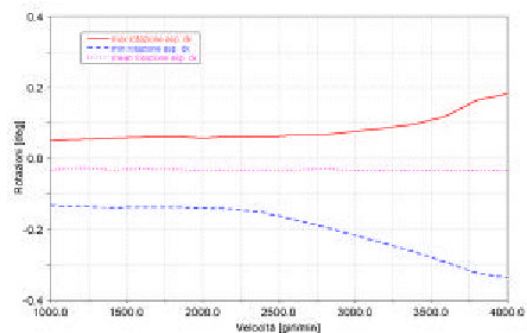


Figure 19 – Amplitude of corresponding torsional oscillations during transient

4.3 Analysis of the transient

Of great interest is the possibility of performing the analyses not only at a pre-determined rotation speed, but also over the transient during which the system is subjected to the most severe operating conditions. From the trend of the moment in the different sections of the shaft, it is possible to identify the critical points where maximum stresses occur. In particular, the greatest stress is always found in the 13th section of the shaft, near the phase converter (Figures 17 and 18). Simulating a transient in acceleration lasting a little less than a second, the amplitude of the torsional oscillations between the shaft extremities (Figure 19) is acceptable at normal

engine speeds, while, as in the case at constant velocity, the system shows vibrational phenomena close to maximum engine speed.

5. CONCLUSIONS

The dynamic behaviour of the timing system was studied on an 8 cylinder, 40 valve internal combustion engine. Multibody models of increasing complexity and FEM models of the various components were used. Static and dynamic experimental trials were conducted: the former with mechanical comparators and strain gauge analyses, the latter by modal analysis. These analyses were then used in validating the numerical models and also provided important information on the internal damping of the system. The dynamic behavior of the, less damped, intake shaft evidenced important torsional vibrations linked to the first natural frequency; these vibrations do not imply appreciable increases in the maximum stresses due to valve operation, nevertheless, the number of cycles to fatigue increases by almost one order of magnitude. The dynamic behavior of the internal springs was also taken into consideration; given that important resonance phenomena occur above 8000 rpm, with one turn of the spring hitting the next, it was suggested that a variable pitch spring be adopted to eliminate this problem.

REFERENCES:

1. G. A. Pignone, U. R. Vercelli, *Motori ad alta potenza specifica*, G.Nada, 1995.
2. D. Noceti, R. Meldolesi, "The use of Valdyn in the design of the valvetrain and timing drive of the new Ferrari V8 Engine", SAE Convention Detroit, March 1999.
3. A Garro, *Progettazione strutturale del motore*, ed. Levrotto & Bella, Torino, 1994.
4. G. Genta, *Principi e Metodologie della Progettazione Meccanica*, ed. Levrotto & Bella, Torino, 1994.
5. M. Geradin, A Cardona, *Flexible multibody dynamics: A Finite Element Approach*, Wiley, New York, 2000.
6. C. Braccesi, F. Cianetti, "Sviluppo dell'interazione tra materiali piezoelettrici e corpi flessibili nella modellazione multibody", *Atti XXVII Convegno Nazionale AIAS*, Perugia, 8-12- Settembre 1998, pp. 337-348.
7. R. Craig, M. C. Bampton, "Coupling of substructures for dynamic analyses", *AIAA Journal*, vol. 6, n.7, (1968).
8. *ADAMS/Solver Subroutines User's Reference manual*, Version 10, Mechanical Dynamics Inc., 1999.
9. *ADAMS/Solver User's Reference manual*, Version 11, Mechanical Dynamics Inc., 2000.
10. *Nastran User's Reference manual*, Version 70.7, MSC Inc., 1999.